X-ray absorption near-edge structures of disordered $Mg_{1-x}Zn_xO$ solid solutions

Teruyasu Mizoguchi,[1,*] Atsuto Seko,[2] Masato Yoshiya,[1,†] Hisao Yoshida,[3] Tomoko Yoshida,[4] W. Y. Ching,[5] and Isao Tanaka[1]

[1]*Department of Materials Science and Engineering, Kyoto University, Sakyo, Kyoto 606-8501, Japan*
[2]*Pioneering Research Unit for Next Generation, Kyoto University, Nishikyo, Kyoto 615-8530, Japan*
[3]*Department of Applied Chemistry, Nagoya University, Nagoya 464-8603, Japan*
[4]*Center for Integrated Research in Science and Engineering, Nagoya University, Nagoya 464-8603, Japan*
[5]*Department of Physics, University of Missouri-Kansas City, Kansas, Missouri 64110-2499, USA*

(Received 26 January 2007; revised manuscript received 1 August 2007; published 28 November 2007)

In order to examine x-ray absorption near-edge structures (XANES) of disordered solid solutions of metal oxides, a combined approach of a first principles supercell method and a cluster expansion method is developed. Zn-L_3 edge XANES are measured on a series of $Mg_{1-x}Zn_xO$ with a rocksalt structure in the range of $x=0.025-0.3$ using synchrotron source. A first principles orthogonalized linear combinations of an atomic orbital method is employed to obtain a theoretical spectrum of a given model. A Zn-2*p* core hole is included in the calculation, and a set of 128 atom supercells is used. Theoretical XANES of disordered solid solutions are obtained as a weighted sum of theoretical spectra for four ordered structures, with the weighting factors determined by the cluster expansion method. The dependence of the spectral shape on the solute concentration is reproduced only when the averaged environment of solute atoms as determined by the solute concentration and the effect of the disordering is taken into account. The formation of the disordered $Mg_{1-x}Zn_xO$ solid solution is confirmed by the Monte Carlo calculations.

DOI: 10.1103/PhysRevB.76.195125 PACS number(s): 71.20.Ps, 78.40.Pg, 61.10.Ht

I. INTRODUCTION

X-ray absorption near-edge structures (XANES) has been widely used to identify the local environment of selected elements.[1,2] Using an advanced synchrotron facility, one can examine most of the elements in the periodic table. XANES can be measured in any kinds of materials, including amorphous or nanosized crystallites with the same quality,[3,4] which is a great advantage beyond diffraction techniques.

Traditionally, the interpretation of XANES has been made by an empirical fingerprinting technique. The spectral shape and energy of a sample are compared to those of references until the best match between them can be found. Recently, first principles methods to compute the theoretical XANES have been developed. Theoretical spectra, which satisfactorily reproduce the experiments, are obtained by introducing core-hole effects to large supercells.[2] In order to use such theoretical technique for the XANES calculation of concentrated solid solutions, an additional tool to model the solid solution is required.

A pioneering work to characterize the atomic arrangement of a solid solution was made by Tatsumi *et al.* on $Si_{6-z}Al_zO_zN_{8-z}$ (sialon) systems.[5] They measured Al *K* edge XANES of β- and γ-phase sialons. Using theoretical fingerprints of many different solute arrangements, they have concluded that the experimental XANES unambiguously indicates that Al solutes are predominantly coordinated by O atoms forming nearest neighbor Al-O bonds. The results were found to be consistent with their first principles energetics.[6] The sialon system exhibits an extreme example showing a strong ordering tendency within the solid solution. The same approach cannot be used for solid solutions showing weak or no ordering tendency.

In the present study, we examine a $Mg_{1-x}Zn_xO$ solid solution with a rocksalt structure. There are four reasons to select this system: (1) Phase diagram is available and a wide range of solid solubility of Zn in MgO has been reported.[7] (2) The formal charge of Zn and Mg is the same, which can eliminate a complexity associated by charge compensation. (3) Ordering tendency in the solid solution was reported to be very weak by first principles calculations.[8] The estimated order-disorder temperature of the most stable ordered structure in the range of $0 \leqslant x \leqslant 0.5$ is only 79 K at $x=0.25$, which implies easiness of forming a disordered structure. (4) High-purity samples can be fabricated in a conventional ceramics laboratory.

First principles calculations of XANES of disordered and concentrated solid solutions require a proper modeling of the atomic arrangements. Computation of a dilute model with just one core-holed solute atom in the supercell is insufficient to reproduce the experimental XANES in general. In order to reproduce the disordered systems, we borrowed an idea of cluster expansion from alloy theory.[9,10] This method successfully reproduced the disorder state in oxide and nitride systems, including MgO-ZnO solid solutions.[11–13] In the present study, theoretical XANES is computed for a number of ordered structures. Then, XANES of disordered structures are constructed by the weighted sum of XANES of ordered structures, with weighting factors obtained by the cluster expansion method. Theoretical results are then compared with experimental ones at several concentrations. To the authors' best knowledge, there has been no such work to combine the cluster expansion and XANES calculations.

II. METHODOLOGY

A. X-ray absorption near-edge structure experiments

High-purity MgO powder (2000A, Ube Materials Industries, Japan) and ZnO powder (Seido Chemical Corp., Japan) were used as starting materials. Both powders were mixed by a magnetic stirrer in warmed ethanol until they dried up. Sintering was carried out in air at 1623 K for 3 h for undoped ZnO and at 1933 K for 2 h for the Zn-doped MgO. The solubility limit of Zn in MgO was reported to be 39 mol % at 1873 K.[7] All samples used in this work were confirmed to be polycrystalline materials with a single crystalline phase of a rocksalt structure by a standard powder x-ray diffraction method. XANES were obtained at BL-7A of the soft x-ray beam line of UVSOR at the Institute for Molecular Science, Okazaki, Japan. Zn-L_3 edge spectra were collected in the total electron yield mode at room temperature using a beryl, $3(BeO)(Al_2O_3)6(SiO_2)$, two-crystal monochromator. The photon energy was calibrated at the Al K edge (1568 eV) from the beryl crystal. Samples were powdered and attached to the first photocathode of the electron multiplier by an adhesive carbon tape in order to minimize surface charging.

B. Computation of x-ray absorption near-edge structures

Theoretical XANES were obtained by a first principles orthogonalized linear combination of atomic orbitals (OLCAO) method with a local-density approximation of density-functional theory.[14] In this method, core orbitals are eliminated from a final secular equation by the orthogonalized process. The orthogonalized process can significantly reduce the computational time and is effective for large systems.[15,16] In the XANES calculation, effects of a core hole that is accompanied by the electron transition process have to be rigorously introduced.[17–19] In order to make the core hole in the OLCAO method, only the core orbital of a core-holed atom is excluded from the orthogonalized process. When we introduce the core hole in the periodic-boundary system, large supercells are indispensable in order to reduce artificial interactions among the core holes in the adjacent cells. It was found that a supercell composed of about 100 atoms is needed for reliable XANES calculations.[20–22] In this study, we employed 108 atoms for w-ZnO and 128 atoms for rock salt-type $Mg_{1-x}Zn_xO$. Both final and ground states were separately calculated. The theoretical transition energy was evaluated by the subtraction of the total energy of the supercell at the ground state from that at the final state.

Basis functions in the OLCAO method are the sum of atomic orbitals, which are expressed using the sets of Gaussian functions.[14] In the self-consistent iteration, a full basis set expansion consisting of atomic orbitals, i.e., 1s, 2s, 2p, 3s, and 3p for O, 1s, 2s, 2p, 3s, 3p, 3d, 4s, and 4p for Mg, and 1s, 2s, 2p, 3s, 3p, 3d, 4s, 4p, 4d, 5s, and 5p for Zn, was employed. After the calculation of the stable electronic structure, partial density of states (PDOS) was obtained by using the minimal basis set, i.e., 1s, 2s, and 2p for O, 1s, 2s, 2p, 3s, 3p, and 3d for Mg, and 1s, 2s, 2p, 3s, 3p, 3d, 4s, 4p, and 4d for Zn. On the other hand, because the XANES structure reflects unoccupied bands in the energy range up to 50 eV higher in energy from the Fermi level, extended basis sets, i.e., [full basis]+ 4s, and 4p for O, [full basis]+4d, 5s, and 5p for Mg, and [full basis]+5d, 6s, and 6p for Zn, were used in the XANES calculations. The selection of those basis functions was the same as previous studies.[2,21,22,27,28]

The photoabsorption cross section (PACS), which is proportional to the electron transition probability, was obtained by calculating the dipole transition matrix between the core orbital of the ground state and the unoccupied bands of the final state. Each PACS was broadened by Gaussian functions of $\Gamma=1.0$ eV. The numbers of k points for the self-consistent calculations, PACS calculations, and PDOS calculations are 4, 8, and 27, respectively. So far, the OLCAO method has been applied to XANES and electron energy loss near-edge structures (ELNES) of many kinds of materials including ceramics, semiconductors, and metals.[2–5,15,16,20–31] It has been known that the present method cannot reproduce the spectrum from strong correlated systems quantitatively[31] and cannot be applied to the $L_{2,3}$ edge of transition metals and the $M_{4,5}$ edge of lanthanides, i.e., "white line," because exact treatments of electron-electron interactions and relativistic effects are indispensable for those spectra.[32–35] However, other spectra, $L_{2,3}$ edges from nontransition metals and K edges from all elements, have been successfully reproduced by the present method.[2–5,15,16,20–30]

Nine different kinds of structures were employed for the XANES calculation. They are isolated Zn in MgO model ($x=0.016$), Zn pair in MgO model ($x=0.031$) at first, second, and third nearest neighbor (NN) cation sites, $2\times2\times2$ superstructure model ($x=0.125$), $L1_2$ model ($x=0.25$), $D0_{22}$ model ($x=0.25$), $L1_1$ model ($x=0.5$), and rocksalt (RS)-ZnO ($x=1$). In order to introduce the core hole correctly, 128-atom supercells were used for all models. Atomic positions were optimized using a plane-wave basis projector augmented wave (PAW)[36,37] method as implemented in the VASP code.[38,39] This method was employed because of its efficiency and accuracy in the structural optimization. The plane-wave cutoff energy was 500 eV, and the number of k points was one in the Brillouin zone for the supercell calculation. Exchange-correlation potential was treated by local-density approximation (LDA).[40,41] Total energies were found to be converged within 5 meV/atom up to the cutoff energy of 800 eV. The error in relative formation energies among the different atomic structures associated with the cutoff energy was found to be less than 1 meV/atom. The relaxation was truncated when the energy gain is less than 1 meV. The relaxed geometries were used for the XANES calculation. When multiple Zn sites are present in the supercell model, the XANES calculations were performed for the individual sites before they are summed to obtain the theoretical spectrum.

C. Computation of disordered structures

In the cluster expansion formalism, the XANES of a structure in a binary system, $I(\varepsilon)$, can be expanded in correlation functions ξ_i, which characterize the structure, as

$$I(\varepsilon) = \sum_{i=1}^{N} \nu_i(\varepsilon)\xi_i, \tag{1}$$

where the coefficient $\nu_i(\varepsilon)$ $(1 \leqslant i \leqslant N)$ is called *effective* cluster interactions (ECI). $\nu_i(\varepsilon)$ can be called effective partial XANES for the ith cluster. Using the general procedure of the structure inversion method[42] to obtain unknown $\nu_i(\varepsilon)$, first principles XANES of the mth ordered structure, $I^{(m)}{}_{\mathrm{FP}}(\varepsilon)(1 \leqslant m \leqslant M)$, is expressed by ECI and the correlation functions as

$$I^{(m)}{}_{\mathrm{FP}}(\varepsilon) = \sum_{i=1}^{N} \nu_i(\varepsilon)\xi_i^{(m)}. \tag{2}$$

It is preferable to select more M structures than N clusters, optimized as the accuracy of the cluster expansion reaches enough level required to predict precise XANES, and obtain $\nu_i(\varepsilon)$ by least squares fitting. However, the procedure should be made for a number of discrete ε points, which is practically very time consuming. In the present study, we have used a simpler approach adopting $N=M$. Then, $\nu_i(\varepsilon)$ can be uniquely determined by multiplying the inverse matrix of ξ_i to both sides of Eq. (1) as

$$\nu_i(\varepsilon) = \sum_{m=1}^{M} I^{(m)}{}_{\mathrm{FP}}(\varepsilon)\{\xi_i^{(m)}\}^{-1}. \tag{3}$$

The theoretical XANES for disordered solid solutions at a given solute concentration, x, i.e., $I^{(\mathrm{dis})}(x,\varepsilon)$, can be given as

$$I^{(\mathrm{dis})}(x,\varepsilon) = \sum_{i=1}^{N} \nu_i(\varepsilon)\xi_i(x)^{(\mathrm{dis})}. \tag{4}$$

Then, we have

$$I^{(\mathrm{dis})}(x,\varepsilon) = \sum_{i=1}^{N}\sum_{m=1}^{M} I^{(m)}{}_{\mathrm{FP}}(\varepsilon)\{\xi_i^{(m)}\}^{-1}\xi_i(x)^{(\mathrm{dis})} = \sum_{m=1}^{M} I^{(m)}{}_{\mathrm{FP}}(\varepsilon)\zeta^{(m)}(x), \tag{5}$$

where

$$\zeta^{(m)}(x) = \sum_{i=1}^{N} \{\xi_i^{(m)}\}^{-1}\xi_i(x)^{(\mathrm{dis})} \tag{6}$$

means the proportion of the mth structure in the disorder solid solution and is simply determined by x. Using Eq. (5), one does not need to compute $\nu_i(\varepsilon)$ explicitly. $I^{(\mathrm{dis})}(x,\varepsilon)$ can be obtained directly from $I^{(m)}{}_{\mathrm{FP}}(\varepsilon)$. In the present study, four ordered models, MgO $(x=0)$, $2\times2\times2$ $(x=0.125)$, $L1_2$ $(x=0.25)$, and $L1_1$ $(x=0.5)$, were used to represent four sets of correlation functions corresponding to the empty, point, first and second NN pairs in the disorder solid solution. $\zeta^{(m)}(x)$ has an analytical form of $4\times(1-2x)^2+8x-3$ for MgO, $-6\times(1-2x)^2-16x+6$ for $2\times2\times2$, and $(1-2x)^2+4x-1$ for both $L1_2$ and $L1_1$. All of these values are positive in the range of x of our interest, i.e., $0 \leqslant x \leqslant 0.3$. Since the set of clusters and ordered models were chosen for simplicity, an increase in N and M was not attempted.

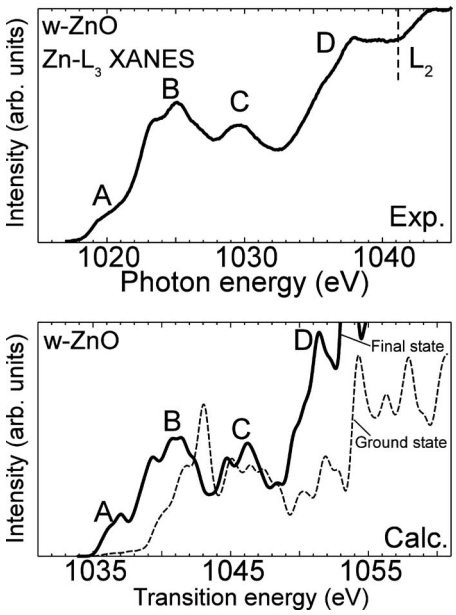

FIG. 1. Experimental and theoretical Zn-L_3 XANES of w-ZnO. The dashed line represents the calculated spectrum at the ground state.

III. RESULTS AND DISCUSSION

A. Comparison of experimental and theoretical spectra

Figure 1 shows experimental and theoretical Zn-L_3 XANES of w-ZnO as a reference material. The spectral shape corresponds to that in a previous ELNES report,[43] except for the fact that the present XANES shows higher energy resolution. Both ground state and final state spectra were calculated. The ground state spectrum was obtained by computing the transition matrix between the core orbital and the unoccupied bands both at the ground state. Features of the calculated spectrum at the final state agree well with those of the experimental spectrum. Error in the transition energy is about 16.0 eV, which is 1.6% of the absolute transition energy. Since the L_2-L_3 splitting for Zn is 23.1 eV,[44] features located at higher energy than peak D can be ascribed to the superposition of L_3 and L_2 components.

A series of Zn-L_3 XANES from $Mg_{1-x}Zn_xO$ solid solutions with different Zn concentrations was displayed in the left panel of Fig. 2. Lower doped samples than 2.5 mol % did not show a sufficient signal to background ratio in the present experimental condition. It should be mentioned that peak A is much stronger than that of the ELNES of the same sample $(x=0.1)$ reported in our previous report.[43] The same tendency can be found in the case of the Mg-$L_{2,3}$ edge of MgO,[45,46] which should be due to better energy resolution in the XANES measurements. In the previous ELNES report, although peak B looked like a single peak due to lower energy resolution,[42] main peak B_1 and subpeak B_2 can be resolved in the present XANES. Spectral features from the solid solutions are clearly different from that of w-ZnO. This

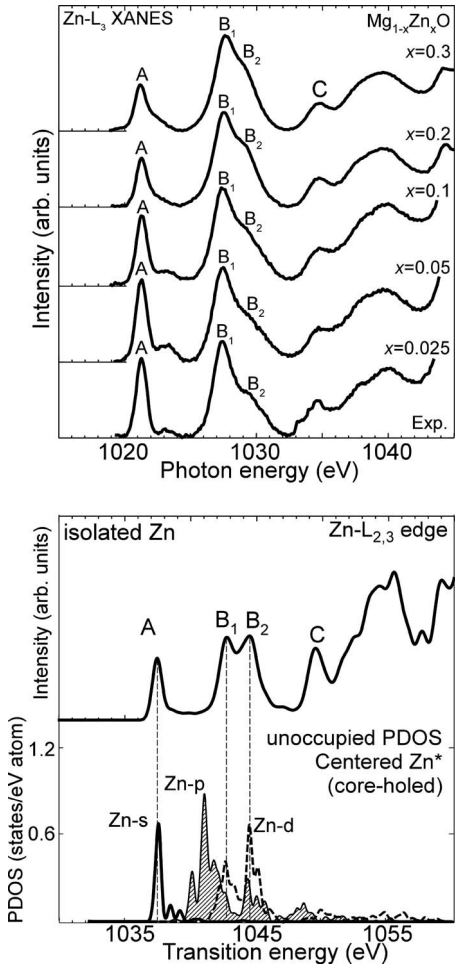

FIG. 2. (Top) Experimental Zn-L_3 XANES from as-sintered $Mg_{1-x}Zn_xO$ solid solutions. (Bottom) Theoretical spectrum from the isolated Zn in MgO and PDOS for the core-holed Zn (Zn^*).

can be ascribed to the difference of the coordination number of Zn.[43] Although the spectral features do not change remarkably even when the Zn concentration is increased by an order of magnitude, a detailed inspection found some features that are dependent on solute concentration. First, the peak intensity ratio of B to A increases with the increase of Zn concentration. Second, subpeak B_2 tends to unite with peak B_1, and they look like a single peak at the high Zn concentration.

The theoretical spectrum of the isolated Zn in the MgO model (x=0.016) is shown in the right panel of Fig. 2, together with theoretical PDOS for the core-holed Zn atom. The magnitude of the energy offset for the theoretical spectra is taken to be the same as the case of w-ZnO. A comparison with PDOS finds that peak A originates from the Zn $2p \rightarrow$ Zn $4s$ transition, whereas peaks B_1 and B_2 are ascribed to the Zn $2p \rightarrow$ Zn $4d$ transition. The presence of peaks A, B_1, B_2, C, and D, and their overall profiles, sharp first peak A, splitting of the second peak to peaks B_1 and B_2, and the presence of peak C followed by broad peaks are found in the theoretical spectrum using the isolated model. However, there are some discrepancies in their fine structures. The largest difference is found for the intensity ratio of B_2 and B_1, i.e., B_2/B_1. B_2/B_1 is close to 1.0, and is nearly doubled in the theoretical spectrum. Considering the fact that the present theoretical methods have been successful for the reproduction of not only peak positions but also peak intensities of XANES in many crystals[2–5,15,16,20–30] including wurtzite ZnO, as shown in Fig. 1, we believe that the disagreement in the shape of peaks B_2 and B_1 is meaningful. The isolated Zn model needs to be modified. In other words, interactions among Zn atoms should be taken into account in order to reproduce the experimental spectra of the solid solutions.

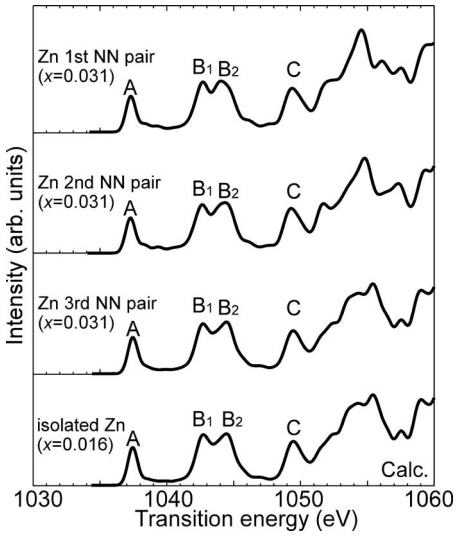

FIG. 3. Theoretical spectra of three kinds of Zn pair models and the isolated Zn model.

B. Effects of Zn arrangements on x-ray absorption near-edge structures

Following the discussion in the previous section, we first examined the effects of paired Zn atoms located at neighboring cationic sites on the theoretical XANES. Three kinds of Zn pairs in a 128-atom supercell are examined. Paired atoms are put at the first, second, and third NN distances. Zn-Zn separations in those models are 2.98, 4.21, and 5.16 Å, respectively. Note that the isolated Zn model in the 128-atom supercell corresponds to Zn pairs at the 14th NN with 11.91 Å Zn-Zn separation. The results of theoretical calculations are shown in Fig. 3. As can be found, spectral shapes are not significantly altered. The spectral feature for the third NN pair is almost identical to that for the isolated one. The magnitude of the agreement cannot be improved merely by forming such pairs. Effects of solute concentration should be properly taken into account.

The second set of calculations was made for five kinds of ordered models, i.e., $2\times2\times2$ (x=0.125), $L1_2$ (x=0.25), $D0_{22}$ (x=0.25), and $L1_1$ (x=0.5). In the $2\times2\times2$ model, all Zn atom pairs are located at the fourth NN sites that are crystallographically identical. Theoretical XANES for the five models are compared to those of the isolated model in Fig. 4. It is interesting that the spectra are similarly composed of peaks A, B_1, B_2, and C in the first 15 eV in all of these models. Up to x=0.5, peaks B_1 and B_2 or their mixture

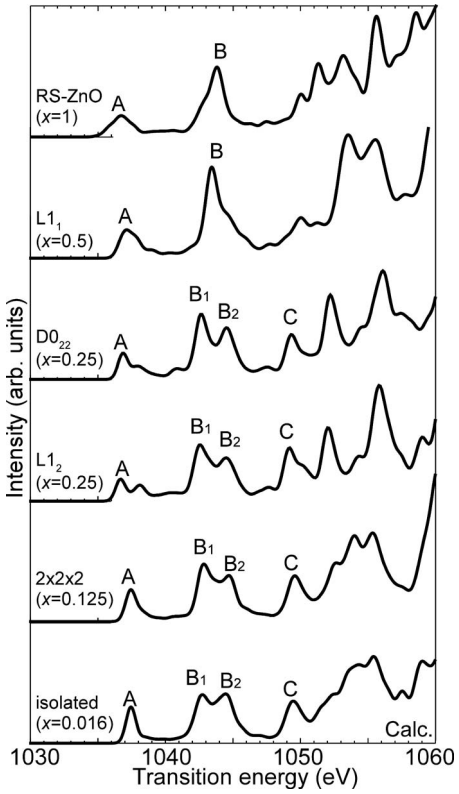

FIG. 4. Theoretical spectra of the ordered $Mg_{1-x}Zn_xO$ models, including RS-ZnO ($x=1$), $L1_1$ ($x=0.5$), $D0_{22}$ ($x=0.25$), $L1_2$ ($x=0.25$), and $2\times2\times2$ ($x=0.125$), and the isolated Zn ($x=0.016$) models.

peak B, tend to become a single peak with the increase of Zn concentration. The ratio A/B also decreases with the Zn concentration. The overall tendencies of the solute concentration dependence of the peak ratios agree with the experimental results. However, it can be seen that those spectra do not reproduce detailed experimental spectra. The discrepancy may be ascribed to the tendency that the $Mg_{1-x}Zn_xO$ forms disordered solid solutions, as predicted by Sanati *et al.*[8] Effects of the disordering should be taken into account, which motivated us to calculate the XANES of the disordered solid solutions.

C. Theoretical x-ray absorption near-edge structures of disordered solid solutions

As described in the methodology chapter, the theoretical XANES of a disordered solid solution can be given by Eq. (5) as a weighted sum of theoretical spectra for the ordered structures. In this study, four ordered models, MgO, $2\times2\times2$, $L1_2$, and $L1_1$ were used to reproduce the disordered structures. The weighting coefficients, given by $\zeta^{(m)}(x)$ in Eq. (5) for four ordered structures, are shown in Fig. 5. The values for $L1_2$ and $L1_1$ are the same. Figure 6 shows the theoretical XANES of disordered solid solutions at five different Zn concentrations. $I_{FP}(\varepsilon)$ by the dilute Zn model ($x=0.031$) was taken as the theoretical XANES of MgO.

As can be seen by a comparison of Figs. 2 and 6, two major features for Zn concentration dependence—i.e., (1)

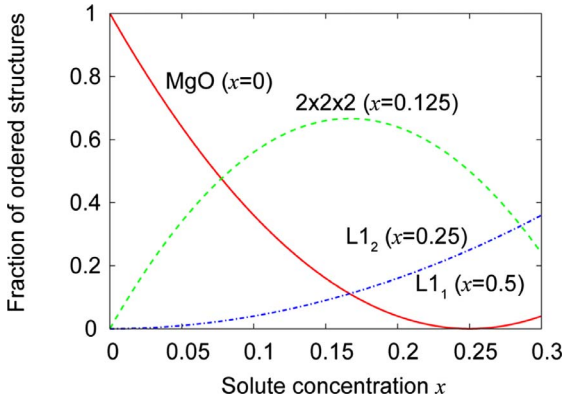

FIG. 5. (Color online) Weighting coefficient $\zeta(x)$ in Eq. (5) for four ordered structures as the function of Zn concentration x. Red (gray) solid line, green (light gray) dashed line, and blue (gray) chain lines represent MgO ($x=0$), $2\times2\times2$ ($x=0.125$), and $L1_2$ ($x=0.25$) and $L1_1$ ($x=0.5$), respectively.

A/B ratio decreases and peak B_2 tends to unite with peak B_1 and (2) the mixture of peaks B_1 and B_2 becomes a single peak when the Zn concentration increases—are reproduced by taking the disordered models into account. It is interesting that the dependence cannot be reproduced merely by using theoretical spectra calculated for Zn pairs, as shown in Fig. 3. Although the present cluster expansion has employed only four clusters, i.e., empty, point, first and second NN pairs, the theoretical spectra for the disordered models show a better agreement to the experimental spectra. This strongly suggests that a proper treatment of highly concentrated solid solution is necessary to reproduce the experimental XANES in the present system. Theoretical spectra shown in Fig. 3 were only for low solute concentrations, i.e., $x=0.016$ and 0.031.

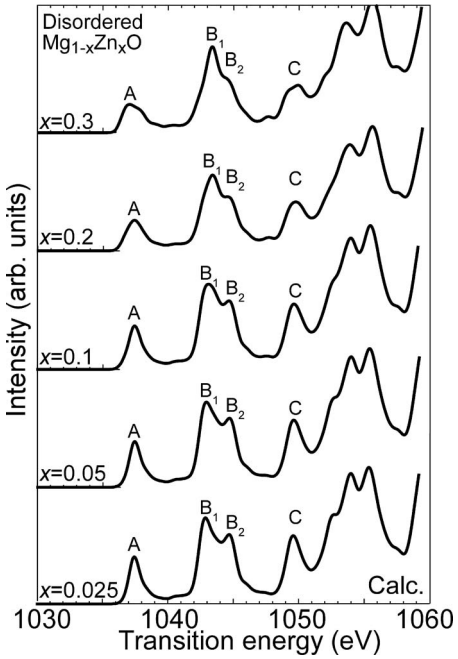

FIG. 6. Theoretical spectra for the disordered $Mg_{1-x}Zn_xO$ solid solution.

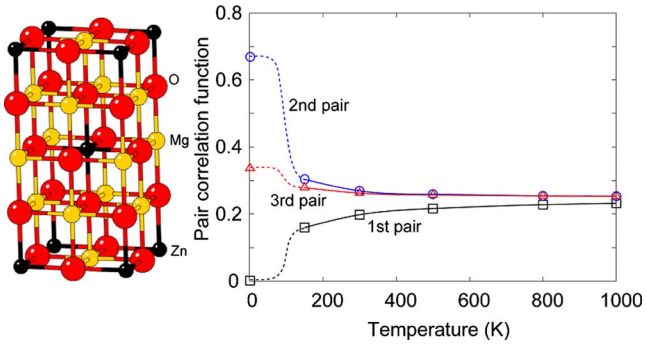

FIG. 7. (Color online) Calculated pair correlation functions with temperatures for $x=0.25$ by Monte Carlo calculations. The ground state structure by the present calculation, namely, the structure at 0 K, was $D0_{22}$, as shown in the left panel. Square, circular, and triangular symbols represent first, second, and third near neighbor pair models, respectively.

D. Confirmation of the disordered solid solution by Monte Carlo calculations

The ordering tendency of the $Mg_{1-x}Zn_xO$ solid solution was reported to be very weak by first principles calculations.[8] They reported that the $D0_{22}$ ($x=0.25$) structure is preferred at the ground state. The estimated order-disorder temperature was 79 K. In the present study, we also made a similar set of calculations in order to confirm their results and variation of the pair correlation functions with temperature. First principles PAW calculations with LDA were made for 34 different kinds of ordered structures. Their energies were expanded with 11 clusters selected among 44 different ones by generic algorithm[47,48] with a mutation rate of 5%, population size of 20, and matings of 6×10^5 times. The resultant cross validation score was 0.318 meV/cation. Then, Monte Carlo (MC) calculations were made using a 3.2×10^4-atom supercell for 2×10^3 MC steps at the given temperatures. Figure 7 shows the computed pair correlation functions with temperatures for $x=0.25$. MC calculations were made in between 150 and 1000 K. Pair correlation functions for the $D0_{22}$ structure are shown together. As can be seen, all four pair correlation functions are already close to the disordered limit at 300 K because the ordering energy is very small. The result is consistent with the work by Sanati *et al.*[8] In this study, we confirmed the disordered $Mg_{1-x}Zn_xO$ solid solutions by using both XANES and the Monte Carlo calculations.

IV. SUMMARY

$Mg_{1-x}Zn_xO$ with a rocksalt structure was used as a model of disordered solid solutions. Their Zn-L_3 XANES were measured in the range of $x=0.025-0.30$ using synchrotron source. First principles calculations were made to reproduce the experimental spectra. Major results can be summarized as follows.

(1) First principles OLCAO calculations were systematically made to obtain theoretical XANES for a given structure. A Zn $2p$ core hole was included into the self-consistent calculation of a supercell composed of more than 100 atoms. The experimental L_3 XANES of w-ZnO was well reproduced.

(2) Although peak positions of the experimental XANES of $Mg_{1-x}Zn_xO$ solid solutions were roughly reproduced by the isolated Zn solute model in MgO using a supercell composed of 128 atoms, small discrepancies were found in the A/B intensity ratio and the shape of peaks B_1 and B_2. It was found that those spectral features are dependent on the Zn concentration.

(3) Two different sets of theoretical XANES were computed by the OLCAO method for models in which atomic positions were optimized by the plane-wave basis PAW method. The first set was composed of Zn pairs at neighboring cationic sites. The theoretical XANES of these models were found to be not significantly different from that of an isolated Zn model. The agreement between theory and experiment was not improved using these pair models. The second set of models was composed of ordered alloy structures within a wide range of Zn concentration. Both the intensity ratios of peaks A/B and the shape of peaks B_1/B_2 showed similar dependency on Zn concentration to those by experiment.

(4) A method to compute the theoretical XANES of solid solutions on the basis of the cluster expansion method was given. Using this method, one can obtain the theoretical XANES of solid solutions as the weighted sum of theoretical spectra for ordered structures. One need not compute effective partial XANES for each cluster, $\nu_i(\varepsilon)$, explicitly. Using theoretical spectra of four ordered structures and four clusters, and adopting the weighting factors, $\zeta^{(m)}(x)$, for the disordered models, the dependence of the spectral shape on the solute concentration was well reproduced. It was thus concluded that the Zn-L_3 XANES of the $Mg_{1-x}Zn_xO$ solid solution is more strongly affected by the averaged environment of solute atoms as determined by the solute concentration rather than the local environment as exemplified by the pair formation.

(5) The weak ordering tendency in the $Mg_{1-x}Zn_xO$ system was confirmed by a detailed cluster expansion analysis combined to Monte Carlo simulation.

ACKNOWLEDGMENTS

This study was supported by a Grant-in-Aid for Scientific Research in Priority Area "Nano Materials Science for Atomic Scale Modification" and the COE program from the Ministry of Education, Sports, and Culture of Japan. T.M. was supported by the JSPS research foundation. A.S. was supported by the Program for Improvement of Research Environment for Young Researchers from Special Coordination Funds for Promoting Science and Technology (SCF) commissioned by the Ministry of Education, Culture, Sports, Science and Technology (MEXT) of Japan. W.Y.C. was supported by U.S. DOE under Grant No. DE-FG02-84ER45170. The authors are grateful to E. Shigemasa and N. Kondo for their help in experimental works at UVSOR/IMR.

*Corresponding author. Present address: Institute of Engineering Innovation, The University of Tokyo, 2–11–16, Yayoi, Bunkyo, Tokyo 113–8656, Japan. mizoguchi@sigma.t.u-tokyo.ac.jp
†Present address: Department of Adaptive Machine Systems, Osaka University, Yamadaoka, Suita, Osaka 565-0871, Japan.

[1] J. Stöhr, *NEXAFS Spectroscopy* (Springer, Berlin, 1992).
[2] I. Tanaka, T. Mizoguchi, and T. Yamamoto, J. Am. Ceram. Soc. **88**, 2013 (2005).
[3] T. Suga, S. Kameyama, S. Yoshioka, T. Yamamoto, I. Tanaka, and T. Mizoguchi, Appl. Phys. Lett. **86**, 163113 (2005).
[4] S. Yoshioka, F. Oba, R. Huang, I. Tanaka, T. Mizoguchi, and T. Yamamoto (unpublished).
[5] K. Tatsumi, T. Mizoguchi, S. Yoshioka, T. Yamamoto, T. Suga, T. Sekine, and I. Tanaka, Phys. Rev. B **71**, 033202 (2005).
[6] K. Tatsumi, I. Tanaka, H. Adachi, and M. Yoshiya, Phys. Rev. B **66**, 165210 (2002).
[7] E. R. Segnit and A. E. Hlland, J. Am. Ceram. Soc. **8**, 409 (1965).
[8] M. Sanati, G. L. W. Hart, and A. Zunger, Phys. Rev. B **68**, 155210 (2003).
[9] J. M. Sanchez, F. Ducastelle, and D. Gratias, Physica A **128**, 334 (1984).
[10] D. de Fontaine, in *Solid State Physics*, edited by H. Ehrenreich and D. Turnbull (Academic, New York, 1994), Vol. 47, pp. 33–176.
[11] A. Seko, F. Oba, A. Kuwabara, and I. Tanaka, Phys. Rev. B **72**, 024107 (2005).
[12] A. Seko, K. Yuge, F. Oba, A. Kuwabara, I. Tanaka, and T. Yamamoto, Phys. Rev. B **73**, 094116 (2006).
[13] A. Seko, K. Yuge, F. Oba, A. Kuwabara, and I. Tanaka, Phys. Rev. B **73**, 184117 (2006).
[14] W. Y. Ching, J. Am. Ceram. Soc. **73**, 3135 (1990).
[15] P. Rulis, W. Y. Ching, and M. Kohyama, Acta Mater. **52**, 3009 (2004).
[16] T. Mizoguchi, T. Sasaki, S. Tanaka, K. Matsunaga, T. Yamamoto, M. Kohyama, and Y. Ikuhara, Phys. Rev. B **74**, 235408 (2006).
[17] I. Tanaka and H. Adachi, Phys. Rev. B **54**, 4604 (1996).
[18] I. Tanaka, H. Araki, M. Yoshiya, T. Mizoguchi, K. Ogasawara, and H. Adachi, Phys. Rev. B **60**, 4944 (1999).
[19] T. Mizoguchi, I. Tanaka, M. Yoshiya, F. Oba, K. Ogasawara, and H. Adachi, Phys. Rev. B **61**, 2180 (2000).
[20] S. D. Mo and W. Y. Ching, Phys. Rev. B **62**, 7901 (2000).
[21] T. Mizoguchi, I. Tanaka, S. Yoshioka, M. Kunisu, T. Yamamoto, and W. Y. Ching, Phys. Rev. B **70**, 045103 (2004).
[22] T. Mizoguchi, K. Tatsumi, and I. Tanaka, Ultramicroscopy **106**, 1120 (2006).
[23] S. D. Mo and W. Y. Ching, Appl. Phys. Lett. **78**, 3809 (2001).
[24] Y. N. Xu, Y. Chen, S. D. Mo, and W. Y. Ching, Phys. Rev. B **65**, 235105 (2002).
[25] W. Y. Ching, S. D. Mo, and Y. Chen, J. Am. Ceram. Soc. **85**, 11 (2002).
[26] T. Mizoguchi, I. Tanaka, M. Kunisu, M. Yoshiya, H. Adachi and W. Y. Ching, Micron **34**, 249 (2003).
[27] I. Tanaka, T. Mizoguchi, M. Matsui, S. Yoshioka, H. Adachi, T. Yamamoto, T. Okajima, M. Umesaki, W. Y. Ching, Y. Inoue, M. Mizuno, H. Araki, and Y. Shirai, Nat. Mater. **2**, 541 (2003).
[28] M. Kunisu, I. Tanaka, T. Yamamoto, T. Suga, and T. Mizoguchi, J. Phys.: Condens. Matter **16**, 3801 (2004).
[29] T. Mizoguchi, M. Sakurai, A. Nakamura, K. Matsunaga, I. Tanaka, T. Yamamoto, and Y. Ikuhara, Phys. Rev. B **70**, 153101 (2004).
[30] W. Y. Ching and P. Rulis, Phys. Rev. B **73**, 045202 (2006).
[31] T. Mizoguchi, J. P. Buban, K. Matsunaga, T. Yamamoto, and Y. Ikuhara, Ultramicroscopy **106**, 92 (2006).
[32] F. M. F. deGroot, J. Electron Spectrosc. Relat. Phenom. **67**, 529 (1994).
[33] K. Ogasawara, T. Iwata, Y. Koyama, T. Ishii, I. Tanaka, and H. Adachi, Phys. Rev. B **64**, 115413 (2001).
[34] H. Ikeno, T. Mizoguchi, Y. Koyama, Y. Kumagai, and I. Tanaka, Ultramicroscopy **106**, 970 (2006).
[35] H. Ikeno, I. Tanaka, Y. Koyama, T. Mizoguchi, and K. Ogasawara, Phys. Rev. B **72**, 075123 (2005).
[36] P. E. Blöchl, Phys. Rev. B **50**, 17953 (1994).
[37] G. Kresse and D. Joubert, Phys. Rev. B **59**, 1758 (1999).
[38] G. Kresse and J. Hafner, Phys. Rev. B **47**, R558 (1993).
[39] G. Kresse and J. Furthmüller, Phys. Rev. B **54**, 11169 (1996).
[40] D. M. Ceperley and B. J. Alder, Phys. Rev. Lett. **45**, 566 (1980).
[41] J. P. Perdew and A. Zunger, Phys. Rev. B **23**, 5048 (1981).
[42] J. W. D. Connolly and A. R. Williams, Phys. Rev. B **27**, 5169 (1983).
[43] T. Mizoguchi, M. Yoshiya M, J. Li, F. Oba, I. Tanaka, and H. Adachi, Ultramicroscopy **86**, 363 (2001).
[44] J. A. Bearden and A. F. Burr, Rev. Mod. Phys. **39**, 125 (1967).
[45] W. L. O'Brien, J. Jia, Q. Y. Dong, T. A. Callcott, D. R. Mueller, D. L. Ederer, and C. C. Kao, Phys. Rev. B **47**, 15482 (1993).
[46] T. Lindner, H. Sauer, W. Engel, and K. Kambe, Phys. Rev. B **33**, 22 (1986).
[47] G. L. W. Hart, V. Blum, M. J. Walorski, and A. Zunger, Nat. Mater. **4**, 391 (2005).
[48] A. Van de Walle, Nat. Mater. **4**, 362 (2005).